Science Translational Medicine
AAAS

The Four-Herb Chinese Medicine PHY906 Reduces Chemotherapy-Induced Gastrointestinal Toxicity

Wing Lam, *et al.*

Sci Transl Med **2**, 45ra59 (2010);
DOI: 10.1126/scitranslmed.3001270

CHEMOTHERAPY

The Four-Herb Chinese Medicine PHY906 Reduces Chemotherapy-Induced Gastrointestinal Toxicity

Wing Lam,[1] Scott Bussom,[1] Fulan Guan,[1] Zaoli Jiang,[1,2] Wei Zhang,[1] Elizabeth A. Gullen,[1] Shwu-Huey Liu,[2] Yung-Chi Cheng[1]*

(Published 18 August 2010; Volume 2 Issue 45 45ra59)

PHY906, a four-herb Chinese medicine formula first described 1800 years ago, decreases gastrointestinal toxicity induced by the chemotherapeutic drug CPT-11 (irinotecan), as shown in a phase I/II clinical study. Similarly, in a murine colon 38 allograft model, PHY906 increased the antitumor activity of CPT-11 while decreasing animal weight loss caused by CPT-11. Here, we have further examined the effect of PHY906 on the intestinal toxicity caused by CPT-11 in mice. PHY906 did not protect against the initial DNA damage and apoptosis triggered by CPT-11 in the intestine, but by 4 days after CPT-11 treatment, PHY906 had restored the intestinal epithelium by promoting the regeneration of intestinal progenitor or stem cells and several Wnt signaling components. PHY906 also potentiated Wnt3a activity in human embryonic kidney–293 cells. Furthermore, PHY906 exhibited anti-inflammatory effects in mice by decreasing the infiltration of neutrophils or macrophages, tumor necrosis factor–α expression in the intestine, and pro-inflammatory cytokine concentrations in plasma. Chemical constituents of PHY906 potently inhibited nuclear factor κB, cyclooxygenase-2, and inducible nitric oxide synthase. Our results show that the herbal medicine PHY906 can counteract the toxicity of CPT-11 via several mechanisms that act simultaneously.

INTRODUCTION

Many effective chemotherapeutics for cancer are burdened by toxicities that can reduce patient quality of life or hinder their effective use. Attempts to eliminate toxicity by using isolated compounds have largely been unsatisfactory, especially for nonhematological toxicities. Herbal medicines, composed of multiple biologically active compounds, are widely claimed to help a variety of diseases. However, they have not been fully accepted by mainstream medicine because of the complex nature of the formulae, as well as a lack of stringent quality control.

PHY906 is derived from the formulation of Huang Qin Tang, which was first described in Chinese canonical medicine about 1800 years ago for the treatment of different gastrointestinal symptoms, including diarrhea, nausea, and vomiting (*1*). PHY906 consists of four herbs: *Glycyrrhiza uralensis* Fisch (G), *Paeonia lactiflora* Pall (P), *Scutelleria baicalensis* Georgi (S), and *Ziziphus jujuba* Mill (Z). PHY906, currently used in clinical and laboratory studies, can be consistently prepared by following stringent manufacturing practices. Consistency among batches of PHY906 can be ensured by multiple quality-control metrics termed PhytomicsQC, in which comprehensive chemical [liquid chromatography–mass spectrometry (LC-MS)] (*2*) and biological fingerprints are correlated with in vivo biological activities to generate a Phytomics Similarity Index (details of PHY906 quality control can be found in the Materials and Methods).

Irinotecan (CPT-11, Camptosar), along with 5-fluorouracil (5-FU) and leucovorin (LV), is used as first-line therapy for the treatment of metastatic colon or rectal carcinoma. CPT-11 is also approved as a second-line therapy for recurrent metastatic colon or rectal carcinoma after 5-FU–based therapy. The side effects of CPT-11 include vomiting, nausea, and diarrhea, which can be serious. Colonic ulceration as a consequence of intestinal cell death and inflammation, often accompanied by gastrointestinal bleeding, has been observed in association with CPT-11 administration (*3*). Currently, loperamide, an opioid receptor agonist, is used as an adjuvant drug for relieving CPT-11–induced diarrhea, frequently without satisfactory outcomes (*4*, *5*). A phase 1/2 randomized double-blind clinical trial was conducted to examine PHY906 as an adjuvant to CPT-11, 5-FU, and LV (5-FU/LV) for treating metastatic colon or rectal carcinoma in chemotherapy-naïve patients. PHY906 treatment resulted in a significant decrease in patient nausea and diarrhea, and no PHY906-associated toxicity was observed. The pharmacokinetics of CPT-11 and 5-FU/LV were unaltered (*6*). A phase 1/2 clinical trial is now in progress for the evaluation of PHY906 as an adjuvant to CPT-11 in second-line therapy for metastatic colorectal carcinoma (*7*). Preclinical studies indicated that PHY906 may enhance the anticancer activity of CPT-11 while decreasing weight loss and mortality (*8*). Here, we used a murine model to study how PHY906 reduces intestinal damage caused by CPT-11.

RESULTS

PHY906 increases the antitumor activity of CPT-11 while decreasing animal weight loss caused by CPT-11

We tested the effect of different dosages of PHY906, given to mice for 4 days [50, 150, and 500 mg/kg and 1 g/kg orally (po), twice per day] at about 10:00 a.m. and 3:00 p.m., and loperamide, an antidiarrheal agent (2 mg/kg po, twice per day, days 0 to 9), on tumor growth and body weight loss after a single CPT-11 treatment [350 mg/kg intraperitoneally (ip), day 0]. On day 0, PHY906 and loperamide were given 30 min before CPT-11 administration. In the control groups, mice were given a vehicle, either phosphate-buffered saline for intraperitoneal administration or water for oral administration. PHY906 by itself did not significantly inhibit tumor growth. PHY906 at doses of 150 mg/kg, 500 mg/kg, and 1 g/kg enhanced the antitumor activity of CPT-11 (all P values < 0.0001) (Fig. 1A). PHY906 at 500 mg/kg and 1 g/kg reduced the body weight loss caused by

[1]Yale University School of Medicine, New Haven, CT 06520, USA. [2]PhytoCeutica Inc., New Haven, CT 06511, USA.
*To whom correspondence should be addressed. E-mail: yccheng@yale.edu

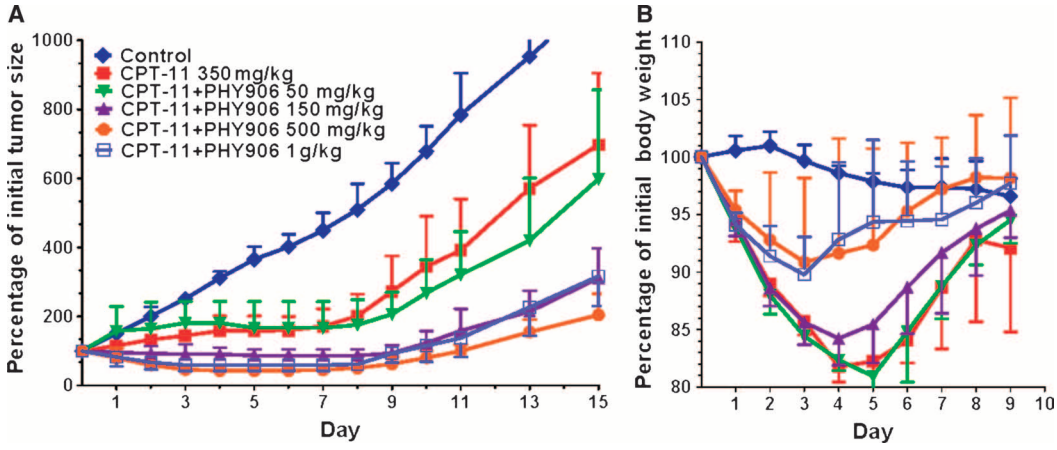

Fig. 1. Effect of PHY906 on the antitumor activity and toxicity of CPT-11. (**A**) Dose effect of PHY906 on the antitumor activity of CPT-11 using the murine colon 38 allograft tumor in BDF1 mice. (**B**) Dose effect of PHY906 in protecting against weight loss induced by CPT-11. CPT-11 (350 mg/kg ip) was injected once on day 0, and PHY906 (50 mg/kg, 125 mg/kg, 500 mg/kg, and 1 g/kg po, twice per day) was administered from day 0 to day 3. Error bars indicate SDs; $n = 5$. Details of experimental procedures are given in Materials and Methods.

CPT-11 (both P values < 0.0001) (Fig. 1B). Compared to PHY906, loperamide did not enhance the antitumor activity of CPT-11 (fig. S1A) and loperamide did not cause body weight recovery until 6 days after CPT-11 treatment (fig. S1B). Because increasing the dose of PHY906 to 1 g/kg or lengthening the treatment duration to 8 days did not improve outcomes (Fig. 1, A and B, and fig. S2, A and B), we focused on PHY906 at 500 mg/kg (twice per day, days 0 to 3) and the results from days 2 and 4 for further detailed analysis.

PHY906 promotes intestinal recovery from damage caused by CPT-11

PHY906 promoted the recovery of histological changes caused by CPT-11. Within 48 hours, a single dose of CPT-11 caused destruction of the jejunum mucosal architecture, in agreement with previous studies (*9*–*11*), and this damage became more pronounced by day 4 (Fig. 2A). On day 2 after CPT-11 treatment, PHY906 had no effect on the damage caused by CPT-11. However, by day 4, the CPT-11/PHY906 group had regained a normal histological structure throughout the small and large intestines (Fig. 2A and fig. S3). This result indicates that PHY906 facilitates the regeneration of intestinal cells after CPT-11–induced damage. Notably, a normal composition of Paneth cells, endocrine cells, and goblet cells could be detected in the CPT-11/PHY906 group, suggesting that PHY906 promotes crypt recovery without affecting normal cell differentiation (Fig. 2B). Treatment with PHY906 alone did not affect intestinal histology on day 2 or 4 (Fig. 2, A and B, and fig. S3).

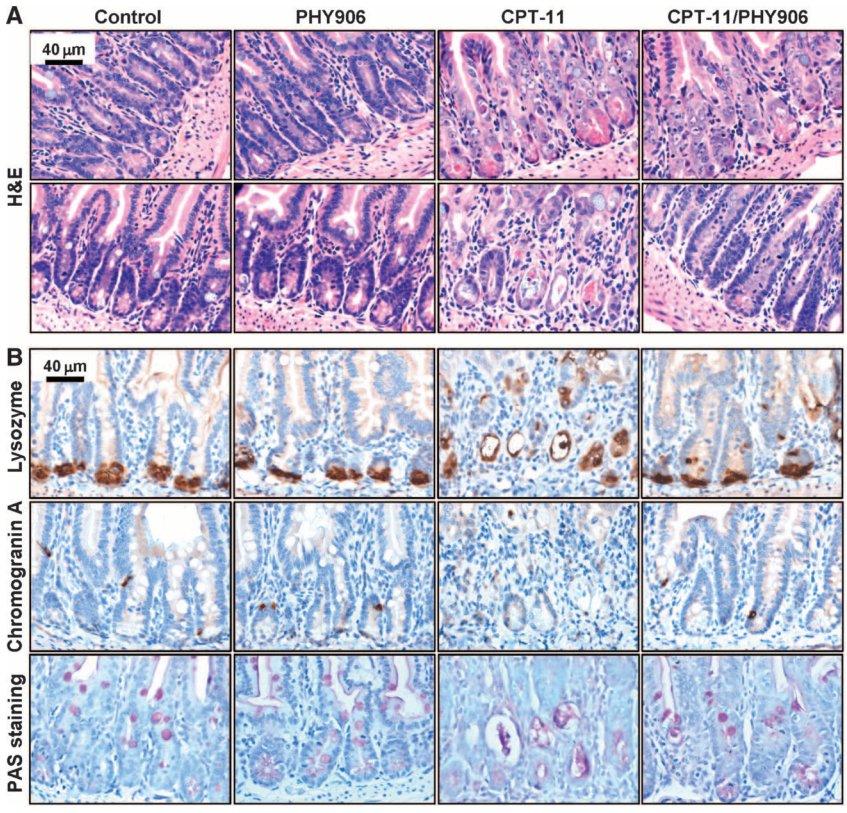

Fig. 2. Effect of PHY906 on CPT-11–induced intestinal damage in mice implanted with murine colon 38 allografts. (**A**) Hematoxylin and eosin (H&E) staining was used to visualize the formalin-fixed sections of the middle jejunum 2 and 4 days after treatment with drug. (**B**) PHY906 promoted the recovery of crypt cells, which displayed normal differentiation after CPT-11 treatment on day 4. Paraffin sections stained for lysozyme (Paneth cells), chromogranin A (endocrine cells), and periodic acid–Schiff (PAS) (goblet cells). Details of the experimental procedures are given in Materials and Methods.

PHY906 decreases apoptotic cells and increases proliferative cells in the intestine after CPT-11 treatment

Terminal deoxynucleotidyl transferase–mediated deoxyuridine triphosphate nick end labeling (TUNEL) results indicated that PHY906 did not prevent the initial DNA damage caused by CPT-11 on day 2 (Fig. 3, A and B, and fig. S4, A and D). By day 4, however, PHY906 had accelerated the disappearance of TUNEL-positive cells in the CPT-11/PHY906 group across all intestinal segments (see P values in Fig. 3B and fig. S4D). Also, on day 4, fewer intestinal apoptotic cells carrying cleaved caspase-3, a sign of apoptosis, were found in the CPT-11/PHY906 group than in the CPT-11 group (fig. S4B).

Proliferative activity in intestinal crypts was estimated by the number of proliferating cell nuclear antigen (PCNA)–positive cells per crypt in different intestinal segments (Fig. 3, C and D, and fig. S4, C and E). CPT-11 significantly reduced the number of proliferative crypt cells on days 2 and 4, particularly at the bottom of the crypts (Fig. 3C and fig. S4C). However, on day 4, the number of crypt-localized PCNA-stained cells in different intestinal segments of the CPT-11/PHY906 group, although comparable to that of control or the PHY906-alone group, was much higher than that of the CPT-11 group ($P < 0.001$ in all intestinal segments; Fig. 3D and fig. S4E). Mitotic and transcriptional activities of the crypt cells were estimated by staining for the phosphorylation of histone H3 at Ser^{10}, acetylation of histone H3 at Lys^{9}, and trimethylation of histone H3 at Lys^{4} (fig. S5). Results from these studies indicated that PHY906 did not prevent the decrease in these activities caused by CPT-11 on day 2. By day 4, however, the mitotic and transcriptional activities of the CPT-11/PHY906 group were comparable to the values in the control or PHY906 group (fig. S5). These results indicated that the recovered crypt cells in the CPT-11/PHY906 group were actively proliferating on day 4.

Bromodeoxyuridine (BrdU) incorporation and BrdU pulse-chase experiments were performed to determine whether the recovery of intestine epithelial cells was due to on-site repair of the damaged cells or replacement with new crypt-generated enterocytes. CPT-11 decreased the number of BrdU-incorporated cells in the crypt area on days 2 and 4 (fig. S6 and Fig. 3F, respectively). In the BrdU pulse-chase experiment, there was faint staining of BrdU of the crypts in the CPT-11 group, implying that the crypt cells had lost their proliferative activities. In contrast to the CPT-11–alone group, a greater number of BrdU-stained cells were found in the CPT-11/PHY906 group on day 4 (Fig. 3E). Moreover, from the BrdU pulse-chase experiment, the presence of stained BrdU cells in the middle of the villi in the CPT-11/PHY906 group suggested that the cells were actively dividing between days 2 and 4 (Fig. 3E). Therefore, the recovered intestinal cells from the CPT-11/PHY906 group on day 4 should represent newly divided crypt-derived progenitor cells. The effect of PHY906 alone did not differ from that in the control group when we used the histological or immunohistological methods described above.

PHY906 promotes the expression of intestinal progenitor or stem cell markers after CPT-11 treatment

To establish whether the repopulated crypt cells in the CPT-11/PHY906 group were intestinal progenitor cells, we stained the cells with antibody to CD44 (*12*). Although PHY906 alone had no effect on the level of CD44, there were fewer CD44-positive cells at the bottom of the crypts after the 2-day CPT-11 or CPT-11/PHY906 treatment (Fig. 4A). However, the number of CD44-positive cells in the CPT-11/PHY906 group was higher than in the CPT-11 group by day 4 (Fig. 4A). Using quantitative real-time polymerase chain reaction (PCR), we further analyzed the messenger RNA (mRNA) expression in the middle jejunum on days 2 and 4 for the recently proposed intestinal stem cell markers Lgr5 (*13*, *14*), Ascl2 (*15*), and Olfm4 (*15*), which are expressed in cycling cells intermingled with Paneth cells, and Bmi1 (*16*), an intestinal stem cell marker for the +4 position of the crypt. PHY906 alone had no effect on the mRNA

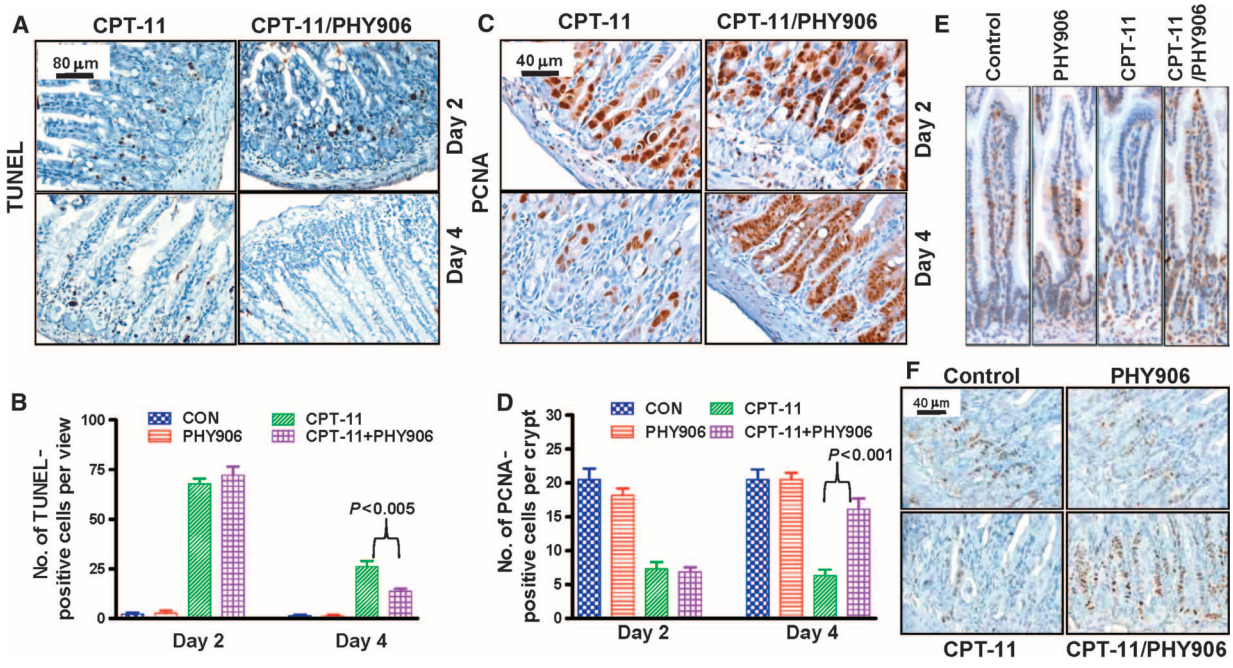

Fig. 3. Effect of PHY906 on DNA damage, expression of PCNA, and incorporation of BrdU after drug treatment in mice implanted with murine colon 38 allografts. (**A** and **B**) TUNEL assay for the detection of DNA breaks in the intestinal cells of middle jejunum sections after drug treatments for 2 and 4 days (three views per sample were counted; $n \geq 8$). (**C** and **D**) PCNA staining per crypt in the middle jejunum sections after drug treatments on days 2 and 4 (three views per sample were counted; $n \geq 8$). (**E**) Migration of BrdU-incorporated cells from crypt to villus in the middle jejunum from day 2 to day 4 [samples were collected 2 days after injection of BrdU (100 mg/kg)]. (**F**) Incorporation of BrdU into the intestinal cells of middle jejunum sections after drug treatments on day 4 [samples were collected 2 hours after injection of BrdU (100 mg/kg)]. Details of the experimental procedures are given in Materials and Methods.

expression of Lgr5, Ascl2, Olfm4, and Bmi1 (Fig. 4, B to E). CPT-11 treatment significantly reduced Lgr5 and Olfm4 expression (Fig. 4, B and D) but had no effect on Ascl2 expression on day 2 (Fig. 4C). The reduction of Lgr5 and Olfm4 mRNA expression caused by CPT-11 was reversed by PHY906 on day 4 ($P = 0.007$ for Lgr5, $P = 0.03$ for Olfm4) (Fig. 4, B and D). PHY906 increased Ascl2 expression after CPT-11 treatment on day 4 ($P = 0.017$) (Fig. 4C). Bmi1 expression was not significantly influenced by PHY906 after CPT-11 treatment (Fig. 4E). In summary, PHY906 induced the expression of the progenitor or stem cell markers CD44, Lgr5, Ascl2, and Olfm4 after CPT-11 treatment. Because CD44, Lgr5, and Ascl2 (*17*) are Wnt-dependent genes and the Wnt signaling pathway is important for stem cell self-renewal and for the proliferation of progenitor cells, we further examined the effect of PHY906 on the mRNA expression of Wnt signaling components. PHY906 increased several of these, including Wnt3 ($P = 0.028$), Fzd5 ($P = 0.049$), Lrp5 ($P = 0.044$), Pygo2 ($P = 0.015$ for day 2 and $P = 0.042$ for day 4), and Axin2 ($P = 0.023$) (fig. S7, A to E), but not β-catenin, Dvl, Gsk3b, Apc, Tcf4, Tle1, Tle2, Bcl9, Bcl9-I, Brg1, Cby1, and Cdc73, 4 days after CPT-11 treatment. These results suggest that PHY906 may promote progenitor cell regeneration after CPT-11 treatment by stimulating Wnt signaling.

β-Glucuronidase–treated PHY906 potentiates Wnt3a activity in the Wnt/β-catenin signaling pathway

We studied whether PHY906 could directly stimulate the Wnt/β-catenin signaling pathway. PHY906 had no appreciable activity in potentiating Wnt3a action at 60 μg/ml and exhibited some inhibition of Wnt signaling at 200 μg/ml in human embryonic kidney (HEK) 293 cells harboring a lymphoid enhancer factor/T cell factor (LEF/TCF) luciferase reporter system (Fig. 5A). PHY906 was subjected to YCC treatment (see Materials and Methods), which includes HCl (which mimics the acidic condition of the stomach) and β-glucuronidase (a major enzyme produced by the bacteria in the gastrointestinal tract). YCC-treated PHY906 can potentiate Wnt3a action to increase the β-catenin–LEF/TCF–mediated transcriptional response three times more than of untreated PHY906 (Fig. 5A), whereas no significant potentiation was observed with a mutated LEF/TCF-binding element (fig. S8A). We deduced that active agents or chemicals for potentiating Wnt3a action are present in S because an amount of YCC-treated S, equivalent to the original amount in PHY906, potentiated Wnt3a action by three times (Fig. 5B), and no potentiation of Wnt3a action was found when S was removed from the four herbs (fig. S8B). As shown in Fig. 5C, HCl-treated S exhibited a dose response similar to that of the untreated S, but β-glucuronidase–treated S responded similarly to YCC-treated S. Overexpression of uridine diphosphate (UDP) glucuronosyltransferases (UGT1A1 or UGT1A9) in the luciferase reporter cell line eliminated the Wnt3a-potentiating activity of PHY906-YCC or S-YCC (Fig. 5, D and E). These results suggest that a compound or compounds lacking glucuronoside(s) are responsible for potentiating Wnt3a action. We further tested the effect of PHY906 on the expression of Axin2, which is a target gene of β-catenin. After YCC treatment, both PHY906 and S potentiated the ability of Wnt3a to induce Axin2 expression in HEK-293 cells (Fig. 5F).

PHY906 inhibits CPT-11–triggered inflammation

As previously reported (*10*, *11*), CPT-11 alone caused pathological changes associated with the infiltration of inflammatory cells (neutrophils and macrophages) and an increase of tumor necrosis factor–α (TNF-α) in the intestine as measured 4 days after treatment (Fig. 6A). Infiltration of the aforementioned inflammatory cells and markers was blocked by PHY906 in the CPT-11/PHY906 group (Fig. 6A). As expected, PHY906 significantly reduced the amount of macrophage chemotactic protein–1 (MCP-1) mRNA ($P = 0.019$) in the middle jejunum tissue and the amount of the proinflammatory cytokines TNF-α ($P = 0.024$) and MCP-1 ($P = 0.016$) in the plasma triggered by CPT-11 on day 4 (Fig. 6, B and C, and fig. S10, A and B). PHY906 also reduced CPT-11–induced inducible nitric oxide synthase (iNOS) mRNA on day

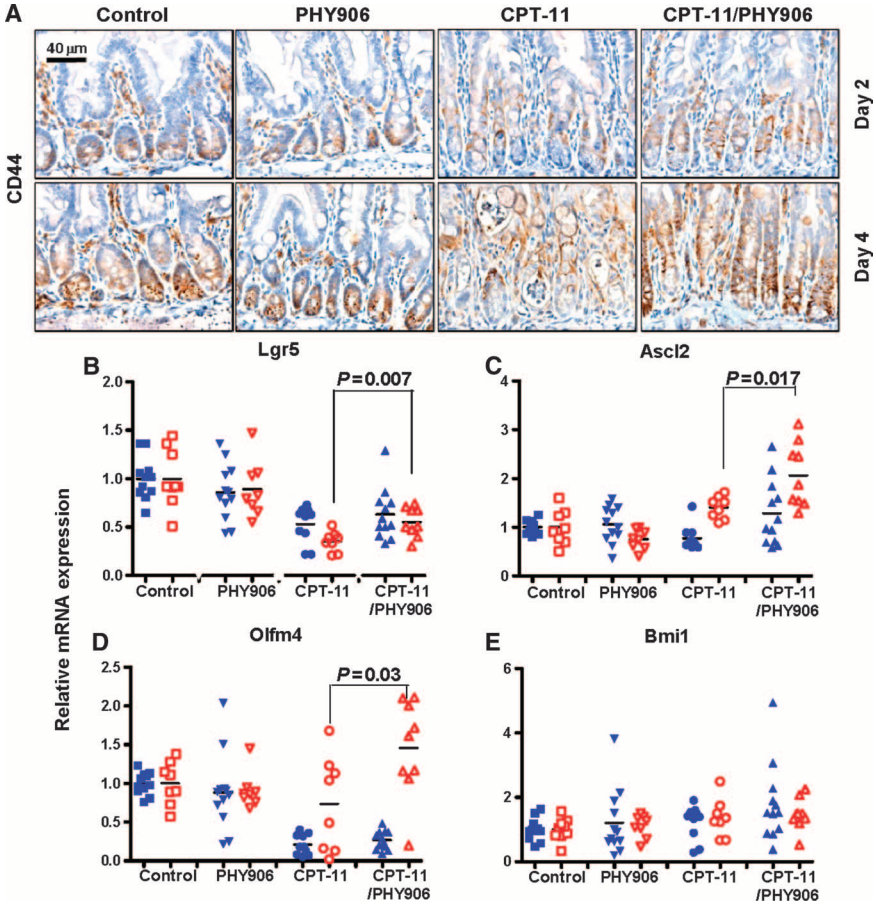

Fig. 4. Effect of PHY906 and/or CPT-11 on the expression of intestinal progenitor or stem cell markers. (**A**) CD44 staining in the middle jejunum sections after drug treatments on days 2 and 4. (**B** to **E**) Quantitative real-time PCR for the mRNA expression of the proposed intestinal stem cell markers Lgr5, Ascl2, Olfm4, and Bmi1 of the middle jejunum on days 2 and 4 after the administration of drug. In (B) to (E), each spot represents the mean of two to three different experiments (triplicate samples of each; $n \geq 8$). Closed blue symbols are results from day 2, and open red symbols are results from day 4. Details of experimental procedures are given in Materials and Methods.

2 ($P = 0.032$) (fig. S9C). Cyclooxygenase-2 (COX-2) mRNA expression was not induced by CPT-11 in our model on day 2 or 4 (fig. S9D). No significant alterations were observed in the chemokine pathways studied [CCL3, CCl4, CCl5, CXCL10, CXCL14, interleukin-18 (IL-18), and IL-1B] in the middle jejunum segments after treatment with CPT-11/PHY906 compared to CPT-11 alone. In cell culture, YCC-treated PHY906 and YCC-treated S had a more pronounced inhibitory effect on TNF-α–induced NF-κB activity than untreated PHY906 ($P < 0.0001$ and $P < 0.0001$, respectively) (Fig. 6D and fig. S10C). PHY906, and the individual components G, P, and S, also inhibited COX-2 in the absence of β-glucuronidase (Fig. 6E and fig. S11). The anti-iNOS activity of PHY906 was reduced by half after YCC treatment ($P = 0.0374$) (Fig. 6F). The anti-iNOS activity of PHY906 was primarily attributed to S, which also reduced anti-iNOS activity after YCC treatment ($P = 0.0086$) (fig. S12C). Because PHY906 directly targets iNOS and COX-2 enzymes, PHY906 may help reduce the downstream inflammatory cascades triggered by iNOS and COX-2.

DISCUSSION

The experimental results presented here, in line with previous observations, support the conclusion that PHY906 can effectively reduce CPT-11–induced gastrointestinal toxicity. CPT-11 is converted into the active metabolite SN38 (7-ethyl-10-hydroxy-camptothecin) by hepatic and intestinal carboxyesterases. Twenty-four hours after administration of CPT-11, SN38 can induce life-threatening diarrhea in patients (*9*). SN38 is metabolized by hepatic UDP glucuronosyltransferase to form an inactive SN38G that is excreted into the bile (*18*, *19*). However, intestinal bacterial β-glucuronidases can transform SN38G back into the active SN38 form that can directly damage the intestine and result in intestinal inflammation. Because PHY906 did not protect against the onset of CPT-11–induced damage in the intestine, it is unlikely that PHY906 glucuronides competed effectively with SN38G for glucuronidases. Our previous pharmacokinetic studies also indicate that PHY906 did not affect the pharmacokinetics of CPT-11, SN38, or SN38G in the plasma of animals (*20*).

Although PHY906 does not protect the intestine from the initial damage caused by CPT-11, PHY906 can effectively inhibit multiple inflammatory markers induced by CPT-11. Unlike single therapeutic agents, PHY906 has multiple sites of action on inflammatory pathways, including TNF-α–induced NF-κB–mediated transcriptional activity and COX-2 and iNOS enzyme activity. Our in vitro experiments showed that YCC treatment enhanced the anti–NF-κB activity of PHY906, suggesting that the active compounds may be aglycone flavonoids. Flavonoids, including baicalein, chrysin, oroxylin A, and wogonin (which are present in both PHY906 and S), have been shown to have anti–NF-κB activity (*21*–*27*). PHY906 also inhibits COX-2 and iNOS, which are downstream of NF-κB and are mediators of gut diarrhea and inflammation (*28*, *29*). Because YCC treatment can decrease

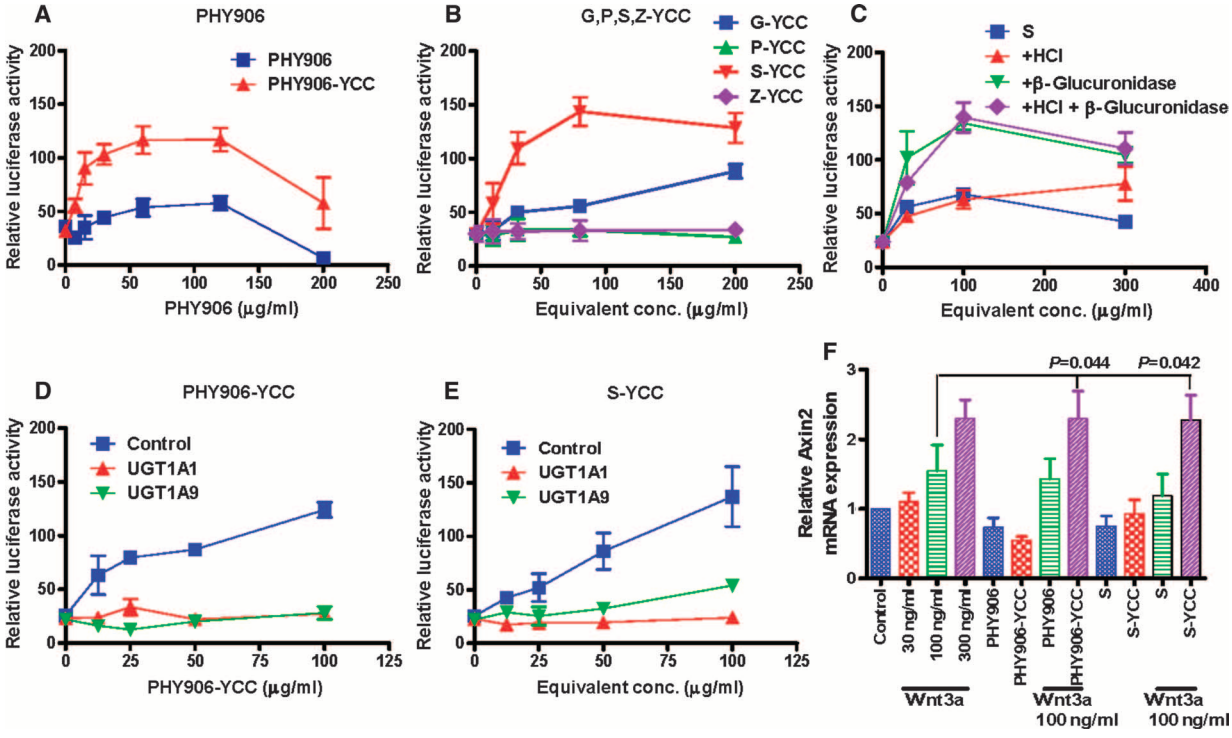

Fig. 5. Effect of β-glucuronidase treatment on PHY906 potentiation of Wnt3a activity of Wnt/β-catenin signaling in HEK-293 cells. HEK-293 cells are stably transfected with a LEF/TCF luciferase reporter plasmid. (**A**) Effects of PHY906 and PHY906-YCC on Wnt/β-catenin signaling. (**B**) Effects of YCC-treated single herbal extraction on Wnt/β-catenin signaling. (**C**) Effects of HCl and β-glucuronidase treatment of S on Wnt3a potentiation. (**D** and **E**) Effects of the overexpression of UGT1A1 and UGT1A9 on the Wnt3a potentiation activity of PHY906-YCC and S-YCC. (**F**) Effect of PHY906 and S (90 μg/ml) on the action of Wnt3a to induce Axin2 expression. Values are means from three to five different experiments (triplicate samples of each); error bars indicate SDs. Details of experimental procedures are given in Materials and Methods.

the inhibitory activity of PHY906 on iNOS, but not on COX-2, it is unlikely that the active compounds within PHY906 that inhibit COX-2 and iNOS are the same.

A notable property of PHY906 is its ability to promote the recovery of damaged intestinal tissue by repopulating progenitor or stem cells and by increasing the proliferating activity of the crypts after CPT-11 treatment. The Wnt-potentiating activity of PHY906 may contribute to this repopulation of crypts cells expressing CD44, Lgr5, and Ascl2 because Wnt/β-catenin signaling is important for stem cell self-renewal and proliferation of progenitor cells in many tissues including the intestine (*30*). Our results are consistent with the results of a study demonstrating modification of Wnt signaling as a strategy to reduce chemotherapy-induced mucosal injury (*31*). That study used a single purified human R-spondin1 protein, which can stimulate Wnt signaling by interfering with DKK1/Kremen-mediated internalization of LRP6 and increasing LRP6 on the cell surface, and showed that it can reduce 5-FU–induced mucositis in vivo (*31*, *32*). In contrast, the mechanism of the Wnt-potentiating activity of PHY906 may involve multiple steps because PHY906 induces several Wnt signaling components after CPT-11 treatment, including Wnt3, Fzd5, Lrp5, and Pygo2. Pygo2 is a coactivator of the β-catenin–TCF complex (*33*) and has been recently suggested to facilitate histone H3 K4 trimethylation (both globally and within the Wnt/β-catenin–targeted loci), which results in expansion of mammary progenitor cells, and to increase histone H3 acetylation, a critical component of spermatogenesis (*34*, *35*). The induction of Pygo2 by PHY906 after CPT-11 treatment sheds lights on why PHY906 increases histone H3 K4 trimethylation and acetylation of intestinal crypt cells after CPT-11 treatment. The Wnt-potentiating activity of PHY906 was enhanced by β-glucuronidase treatment and inhibited by overexpression of UDP glucuronosyltransferases. These results suggest that Wnt signaling in tissues with different β-glucuronidase/UDP glucuronosyltransferase ratios will be differentially affected by PHY906. PHY906 is administered orally and therefore is exposed to intestinal bacteria that express β-glucuronidase, which probably uncovers the Wnt-potentiating activity of PHY906. We suspect that the treatment for 4 days with PHY906 alone did not affect the intestinal progenitor

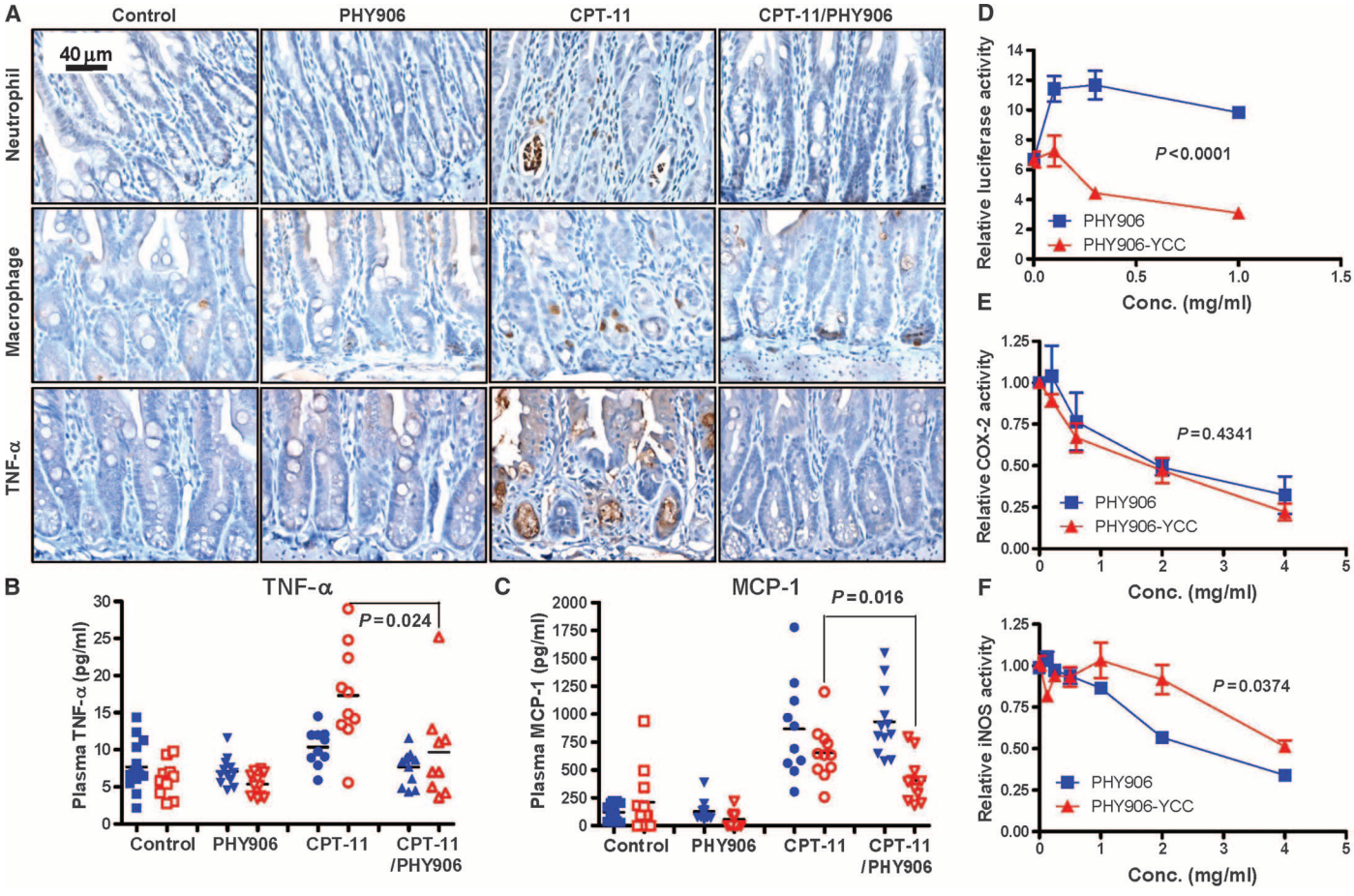

Fig. 6. Effect of PHY906 on the inflammation triggered by CPT-11 in the murine colon 38 allograft–implanted BDF1 mouse model. (**A**) Neutrophil and macrophage infiltration and TNF-α expression in the middle jejunum section 4 days after treatment. (**B** and **C**) Detection of TNF-α and MCP-1 protein in the plasma on posttreatment days 2 and 4. In (B) and (C), each spot represents the mean from two to three different experiments (triplicate samples of each; $n \geq 8$). Closed blue symbols are results from day 2, and open red symbols are results from day 4. (**D**) Inhibitory activity of PHY906 on the TNF-α–induced, NF-κB–mediated transcriptional activity. (**E** and **F**) Inhibitory activity of PHY906 on COX-2 and iNOS enzyme activity. In (D) to (F), values are means from three different experiments (triplicate samples of each); error bars indicate SDs. *P* values in each graph were analyzed by two-way ANOVA for comparing the difference of the dose-response curves. Details of experimental procedures are given in Materials and Methods.

cell growth because negative feedback mechanisms prevent outgrowth of progenitor cells under normal conditions.

In summary, we report that PHY906, a four-herb formulation, reduced the gastrointestinal toxicity of CPT-11 through multiple mechanisms of action that included inhibition of multiple steps of inflammation and the promotion of intestinal progenitor cell repopulation. The development of such multicomponent herbal medicines capable of targeting multiple sites could be useful for future drug discovery and the potential management of complicated diseases. Additionally, mechanistic studies and identification of active compounds could lead to new discoveries in biological and biomedical sciences.

MATERIALS AND METHODS

PHY906 is manufactured to ensure the preparation is of high quality (Supplementary Material). The detailed quality-control methodology PhytomicsQC is described elsewhere (*36*, *37*). Murine colon 38 cells were transplanted subcutaneously into 4- to 6-week-old female BDF1 mice (Charles River Laboratories). After 10 to 14 days, mice with tumor sizes of 150 to 300 mm^3 were selected. PHY906 was given for 4 days (500 mg/kg po, twice per day), and CPT-11 (350 mg/kg ip) was administered on day 0. On day 0, PHY906 was given 30 min before CPT-11 administration. Mice (BDF1 bearing colon 38 tumors) were killed by cervical dislocation 2 or 4 days after initiation of drug treatment. Intestinal and colon tissues were removed, fixed in formalin, embedded in paraffin, and sectioned at 10 μm. Immunohistochemistry was used to detect protein expression of the intestinal tissues. Apoptosis was quantified by the TUNEL assay for detecting DNA breaks in the cells of the intestinal tissues. Quantitative real-time reverse transcription PCR (RT-PCR) was used to quantify mRNA expression. Luciferase reporter assay was used to study the β-catenin/TCF–mediated transcriptional activity. Cytokines in the plasma were measured with the BD Cytometric Bead Array. The prostanoid product of the COX-2 activity assay was quantified by LC-MS. iNOS activity was measured by a colorimetric nitrite assay. Data were analyzed by one- or two-way analysis of variance (ANOVA) (GraphPad Prism 4), Student's *t* test (Microsoft Office Excel), and correlation analysis (GraphPad Prism 4). The difference was considered to be statistically significant when $P < 0.05$.

SUPPLEMENTARY MATERIAL

www.sciencetranslationalmedicine.org/cgi/content/full/2/45/45ra59/DC1
Materials and Methods
Fig. S1. Effect of PHY906 and loperamide on the antitumor activity and animal toxicity of CPT-11.
Fig. S2. Effect of PHY906 treatment duration on the antitumor activity and animal toxicity of CPT-11.
Fig. S3. Hematoxylin and eosin staining of middle jejunum sections from sample collected at days 2 and 4 after drug treatments.
Fig. S4. Apoptosis and proliferation of intestinal cells after drug treatment.
Fig. S5. Immunohistochemical staining for phosphorylation of histone H3 at Ser^{10}, acetylation of histone H3 at Lys^9, and trimethylation of histone H3 at Lys^4 of middle jejunum sections.
Fig. S6. Incorporation of BrdU into the intestinal cells of middle jejunum sections after drug treatment on day 2.
Fig. S7. Effect of drug treatment on the expression of genes of Wnt/β-catenin signaling.
Fig. S8. Effect of PHY906 on Wnt3a activity of Wnt/β-catenin signaling in HEK-293 cells.
Fig. S9. Expression of genes for inflammation after drug treatment.
Fig. S10. Effect of PHY906 on NF-κB–mediated transcriptional activity.
Fig. S11. Effect of PHY906 on COX-2 enzyme activity.
Fig. S12. Effect of PHY906 on iNOS enzyme activity.
Table S1. Quantitative real-time PCR primers.

REFERENCES AND NOTES

1. H.-Y. Hsu, C.-S.Hsu, *Commonly Used Chinese Herb Formulas with Illustrations* (Oriental Healing Art Institute, Long Beach, CA, 1980).
2. M. Ye, S. H. Liu, Z. Jiang, Y. Lee, R. Tilton, Y. C. Cheng, Liquid chromatography/mass spectrometry analysis of PHY906, a Chinese medicine formulation for cancer therapy. *Rapid Commun. Mass Spectrom.* **21**, 3593–3607 (2007).
3. J. R. Hecht, Gastrointestinal toxicity of irinotecan. *Oncology* **12**, 72–78 (1998).
4. D. Abigerges, J. P. Armand, G. G. Chabot, L. Da Costa, E. Fadel, C. Cote, P. Hérait, D. Gandia, Irinotecan (CPT-11) high-dose escalation using intensive high-dose loperamide to control diarrhea. *J. Natl. Cancer Inst.* **86**, 446–449 (1994).
5. D. Cunningham, S. Pyrhönen, R. D. James, C. J. Punt, T. F. Hickish, R. Heikkila, T. B. Johannesen, H. Starkhammar, C. A. Topham, L. Awad, C. Jacques, P. Herait, Randomised trial of irinotecan plus supportive care versus supportive care alone after fluorouracil failure for patients with metastatic colorectal cancer. *Lancet* **352**, 1413–1418 (1998).
6. M. P. Farrell, S. Kummar, Phase I/IIA randomized study of PHY906, a novel herbal agent, as a modulator of chemotherapy in patients with advanced colorectal cancer. *Clin. Colorectal Cancer* **2**, 253–256 (2003).
7. National Clinical Trial Number 00730158.
8. S.-H. Liu, Z. Jiang, T.-M. Su, W.-Y. Gao, C.-H. Leung, Y. Lee, Y.-C. Cheng, Developing PHY906 as a broad-spectrum modulator of chemotherapeutic agents in cancer therapy. *Proc. Am. Assoc. Cancer Res.* **45**, 128 (2004).
9. N. Ikuno, H. Soda, M. Watanabe, M. Oka, Irinotecan (CPT-11) and characteristic mucosal changes in the mouse ileum and cecum. *J. Natl. Cancer Inst.* **87**, 1876–1883 (1995).
10. J. Zhao, L. Huang, N. Belmar, R. Buelow, T. Fong, Oral RDP58 allows CPT-11 dose intensification for enhanced tumor response by decreasing gastrointestinal toxicity. *Clin. Cancer Res.* **10**, 2851–2859 (2004).
11. M. L. Melo, G. A. Brito, R. C. Soares, S. B. Carvalho, J. V. Silva, P. M. Soares, M. L. Vale, M. H. Souza, F. Q. Cunha, R. A. Ribeiro, Role of cytokines (TNF-α, IL-1β and KC) in the pathogenesis of CPT-11-induced intestinal mucositis in mice: Effect of pentoxifylline and thalidomide. *Cancer Chemother. Pharmacol.* **61**, 775–784 (2008).
12. V. J. Wielenga, R. Smits, V. Korinek, L. Smit, M. Kielman, R. Fodde, H. Clevers, S. T. Pals, Expression of CD44 in *Apc* and *Tcf* mutant mice implies regulation by the WNT pathway. *Am. J. Pathol.* **154**, 515–523 (1999).
13. N. Barker, J. H. van Es, J. Kuipers, P. Kujala, M. van den Born, M. Cozijnsen, A. Haegebarth, J. Korving, H. Begthel, P. J. Peters, H. Clevers, Identification of stem cells in small intestine and colon by marker gene *Lgr5*. *Nature* **449**, 1003–1007 (2007).
14. T. Sato, R. G. Vries, H. J. Snippert, M. van de Wetering, N. Barker, D. E. Stange, J. H. van Es, A. Abo, P. Kujala, P. J. Peters, H. Clevers, Single Lgr5 stem cells build crypt–villus structures *in vitro* without a mesenchymal niche. *Nature* **459**, 262–265 (2009).
15. L. G. van der Flier, M. E. van Gijn, P. Hatzis, P. Kujala, A. Haegebarth, D. E. Stange, H. Begthel, M. van den Born, V. Guryev, I. Oving, J. H. van Es, N. Barker, P. J. Peters, M. van de Wetering, H. Clevers, Transcription factor achaete scute-like 2 controls intestinal stem cell fate. *Cell* **136**, 903–912 (2009).
16. E. Sangiorgi, M. R. Capecchi, *Bmi1* is expressed *in vivo* in intestinal stem cells. *Nat. Genet.* **40**, 915–920 (2008).
17. L. G. Van der Flier, J. Sabates-Bellver, I. Oving, A. Haegebarth, M. De Palo, M. Anti, M. E. Van Gijn, S. Suijkerbuijk, M. Van de Wetering, G. Marra, H. Clevers, The intestinal Wnt/TCF signature. *Gastroenterology* **132**, 628–632 (2007).
18. L. P. Rivory, M. R. Bowles, J. Robert, S. M. Pond, Conversion of irinotecan (CPT-11) to its active metabolite, 7-ethyl-10-hydroxycamptothecin (SN-38), by human liver carboxylesterase. *Biochem. Pharmacol.* **52**, 1103–1111 (1996).
19. R. Humerickhouse, K. Lohrbach, L. Li, W. F. Bosron, M. E. Dolan, Characterization of CPT-11 hydrolysis by human liver carboxylesterase isoforms hCE-1 and hCE-2. *Cancer Res.* **60**, 1189–1192 (2000).
20. M. Ye, Z. Jiang, W. Lam, G. Dutschman, S. Bussom, P. C. Chen, S. H. Liu, Y. C. Cheng, A novel herb-drug interaction: Irinotecan can significantly change the pharmacokinetics and pharmacodynamics of PHY906, a Chinese medicine formulation for cancer therapy. *Proc. Am. Assoc. Cancer Res.* **49** (2008).
21. Y. Chen, L. Yang, T. J. Lee, Oroxylin A inhibition of lipopolysaccharide-induced iNOS and COX-2 gene expression via suppression of nuclear factor-κβ activation. *Biochem. Pharmacol.* **59**, 1445–1457 (2000).
22. Y. C. Chen, S. C. Shen, L. G. Chen, T. J. Lee, L. L. Yang, Wogonin, baicalin, and baicalein inhibition of inducible nitric oxide synthase and cyclooxygenase-2 gene expressions in-

duced by nitric oxide synthase inhibitors and lipopolysaccharide. *Biochem. Pharmacol.* **61**, 1417–1427 (2001).
23. Y. S. Chi, B. S. Cheon, H. P. Kim, Effect of wogonin, a plant flavone from *Scutellaria radix*, on the suppression of cyclooxygenase-2 and the induction of inducible nitric oxide synthase in lipopolysaccharide-treated RAW 264.7 cells. *Biochem. Pharmacol.* **61**, 1195–1203 (2001).
24. B. Y. Kang, S. W. Chung, S. H. Kim, D. Cho, T. S. Kim, Involvement of nuclear factor-κβ in the inhibition of interleukin-12 production from mouse macrophages by baicalein, a flavonoid in *Scutellaria baicalensis*. *Planta Med.* **69**, 687–691 (2003).
25. C. C. Lin, D. E. Shieh, The anti-inflammatory activity of *Scutellaria rivularis* extracts and its active components, baicalin, baicalein and wogonin. *Am. J. Chin. Med.* **24**, 31–36 (1996).
26. I. Wakabayashi, K. Yasui, Wogonin inhibits inducible prostaglandin E_2 production in macrophages. *Eur. J. Pharmacol.* **406**, 477–481 (2000).
27. D. Y. Zhang, J. Wu, F. Ye, L. Xue, S. Jiang, J. Yi, W. Zhang, H. Wei, M. Sung, W. Wang, X. Li, Inhibition of cancer cell proliferation and prostaglandin E_2 synthesis by *Scutellaria baicalensis*. *Cancer Res.* **63**, 4037–4043 (2003).
28. Y. Kase, T. Hayakawa, Y. Togashi, T. Kamataki, Relevance of irinotecan hydrochloride-induced diarrhea to the level of prostaglandin E_2 and water absorption of large intestine in rats. *Jpn. J. Pharmacol.* **75**, 399–405 (1997).
29. B. J. Whittle, Nitric oxide-modulating agents for gastrointestinal disorders. *Expert Opin. Investig. Drugs* **14**, 1347–1358 (2005).
30. T. Fevr, S. Robine, D. Louvard, J. Huelsken, Wnt/β-catenin is essential for intestinal homeostasis and maintenance of intestinal stem cells. *Mol. Cell. Biol.* **27**, 7551–7559 (2007).
31. K. A. Kim, M. Kakitani, J. Zhao, T. Oshima, T. Tang, M. Binnerts, Y. Liu, B. Boyle, E. Park, P. Emtage, W. D. Funk, K. Tomizuka, Mitogenic influence of human R-spondin1 on the intestinal epithelium. *Science* **309**, 1256–1259 (2005).
32. M. E. Binnerts, K. A. Kim, J. M. Bright, S. M. Patel, K. Tran, M. Zhou, J. M. Leung, Y. Liu, W. E. Lomas III, M. Dixon, S. A. Hazell, M. Wagle, W. S. Nie, N. Tomasevic, J. Williams, X. Zhan, M. D. Levy, W. D. Funk, A. Abo, R-Spondin1 regulates Wnt signaling by inhibiting internalization of LRP6. *Proc. Natl. Acad. Sci. U.S.A.* **104**, 14700–14705 (2007).
33. B. Thompson, F. Townsley, R. Rosin-Arbesfeld, H. Musisi, M. Bienz, A new nuclear component of the Wnt signalling pathway. *Nat. Cell Biol.* **4**, 367–373 (2002).
34. B. Gu, P. Sun, Y. Yuan, R. C. Moraes, A. Li, A. Teng, A. Agrawal, C. Rhéaume, V. Bilanchone, J. M. Veltmaat, K. Takemaru, S. Millar, E. Y. Lee, M. T. Lewis, B. Li, X. Dai, Pygo2 expands mammary progenitor cells by facilitating histone H3 K4 methylation. *J. Cell Biol.* **185**, 811–826 (2009).
35. M. Nair, I. Nagamori, P. Sun, D. P. Mishra, C. Rhéaume, B. Li, P. Sassone-Corsi, X. Dai, Nuclear regulator Pygo2 controls spermiogenesis and histone H3 acetylation. *Dev. Biol.* **320**, 446–455 (2008).
36. M. W. Saif, F. Lansigan, S. Ruta, L. Lamb, M. Mezes, K. Elligers, N. Grant, Z. L. Jiang, S. H. Liu, Y. C. Cheng, Phase I study of the botanical formulation PHY906 with capecitabine in advanced pancreatic and other gastrointestinal malignancies. *Phytomedicine* **17**, 161–169 (2010).
37. R. Tilton, A. Paiva, J. Guan, R. Marathe, Z. Jiang, W. van Eyndhoven, Z. Prusoff, J. Bjoraker, H. Wang, S. Liu, Y. C. Cheng, PhytomicsQC: A comprehensive platform for quality control of botanical drugs—a case study of PHY906. *Chinese Med.*, **5**, 30 (2010).
38. **Acknowledgments:** We thank Y. Cheng, S. Lin, and C. J. Qu for critical reading of the manuscript. **Funding:** Supported in part by grant UO-63477 from the National Cancer Institute and NIH. Y.-C.C. is a Fellow of the National Foundation for Cancer Research. **Author contributions:** W.L. performed the experiments (tissue preparation, immunohistochemistry, quantitative RT-PCR, luciferase reporter construction, iNOS assay, and COX-2 assay) and wrote the paper. S.B. performed the experiments (tissue preparation, RNA extraction, quantitative RT-PCR, and cytokine assay) and wrote the paper. F.G. performed the experiments (tissue preparation, immunohistochemistry, iNOS assay, and COX assay). Z.J. performed all animal experiments. W.Z. performed LC-MS analysis. E.A.G. performed the luciferase assay. S.-H.L. provided PHY906, quality control information, and discussion. Y.-C.C. designed the experiments and wrote the paper. **Competing interests:** Y.-C.C. is a scientific founder of and has equity interest in PhytoCeutica Inc., a company that develops traditional Chinese medicine into drugs for the treatment of cancer and that licenses PHY906 from Yale University. Z.J. and S.-H.L. own stock in PhytoCeutica Inc. Yale University holds a patent on the herbal composition PHY906 and its use in chemotherapy. **Accession numbers:** National Clinical Trial Number 00730158.

Submitted 10 May 2010
Accepted 30 July 2010
Published 18 August 2010
10.1126/scitranslmed.3001270

Citation: W. Lam, S. Bussom, F. Guan, Z. Jiang, W. Zhang, E. A. Gullen, S.-H. Liu, Y.-C. Cheng, The four-herb Chinese medicine PHY906 reduces chemotherapy-induced gastrointestinal toxicity. *Sci. Transl. Med.* **2**, 45ra59 (2010).